JACS
JOURNAL OF THE AMERICAN CHEMICAL SOCIETY

COMMUNICATION

pubs.acs.org/JACS

Electrostatic Control of Lipid Bilayer Self-Spreading Using a Nanogap Gate on a Solid Support

Yoshiaki Kashimura,* Kazuaki Furukawa, and Keiichi Torimitsu

NTT Basic Research Laboratories, NTT Corporation, Atsugi 243-0198, Japan

Supporting Information

ABSTRACT: We have demonstrated for the first time that the self-spreading of supported lipid bilayers can be controlled by the temporal switching of an electric field applied between nanogap electrodes. To account for this phenomenon, we propose an electrostatic trapping model in which an electric double layer plays an important role. The validity of this mechanism was verified by the dependence of self-spreading on the nanogap width and the ionic concentration of the electrolyte. Our results provide a promising tool for the temporal and spatial control of lipid bilayer formation for nanobio devices.

A cell membrane is dynamic and routinely transports membrane components such as proteins, leading to its biological functionality. A lipid bilayer on a solid support, which can be regarded as a model cell membrane, retains many of the structural and physical properties of a cell membrane.[1] Accordingly, control of the motion of such supported lipid bilayers (SLBs) and the membrane-embedded species is a significant subject in regard to further understanding of many cellular processes and applications in biophysics and bioanalytical chemistry. The application of an external electric field is an effective way of spatially controlling the specific lipid molecules embedded in an SLB.[2] When the external electric field (10−100 V/cm) is applied tangentially to an SLB on a patterned surface, charged lipid molecules and membrane associated proteins are reorganized by electrophoretic and electroosmotic forces, respectively, leading to steady-state concentration gradients.[3] These concentration gradients result from the competition between the diffusive mixing and field-induced motion of the charged molecules. Some interesting work, such as the Brownian ratchet[4] and molecular manipulation and separation,[5] using these electric field effects has been reported. In regard to other attempts, we demonstrated the spatial control of SLB formation by employing the self-spreading method on a patterned substrate.[6] Self-spreading is a characteristic of an SLB that results from its spontaneous growth.[7] An SLB works as a molecular transport medium. The molecular filtering of dye-conjugated lipid molecules embedded in an SLB was achieved using the self-spreading method on a substrate with a periodic array of nanogap gates with widths between 75 and 500 nm.[8] We also fabricated a microchannel device to detect fluorescence resonance energy transfer.[9] Furthermore, we investigated the effect of a sub-100-nm nanogap structure on the molecular dynamics of a self-spreading SLB.[10] Despite these efforts, controlling the motion of SLBs temporally and spatially remains a challenge.

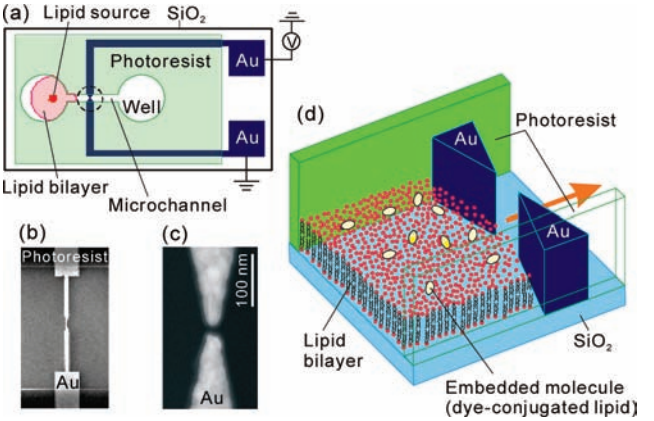

Figure 1. (a) Schematic diagram of the device. A microchannel and wells were formed on a gold nanogap structure using an organic photoresist. At the beginning of the experiment, a lipid source was fixed inside one well and immersed in a buffer solution. (b) Magnified view of the device around a nanogap. (c) Scanning electron microscope image of a nanogap. (d) Illustration of the region around the nanogap during operation.

In this communication, we describe a new method for the temporal and spatial control of SLB formation using a nanogap gate in conjunction with an external direct current (DC) electric field. For this purpose, we employed the device structure illustrated in Figure 1. A pair of electrodes with a separation of less than 100 nm was fabricated using Au/Ti (30 nm/1 nm) on a hydrophilic SiO_2 surface. A 10 μm wide, 1 μm high microchannel with wells at both ends was fabricated on this nanogap structure using a hydrophobic organic photoresist. A lipid mixture consisting of uncharged L-α-phosphatidylcholine (Egg-PC) and negatively charged L-α-phosphatidylglycerol (Egg-PG) containing 1 mol % Texas Red−DHPE[11] was attached to one of the wells. The self-spreading of the SLBs was initiated by immersing the substrate gently in a buffer solution consisting of 10 mM Tris-HCl + 100 mM NaCl (pH 7.6). An Egg-PC:Egg-PG molar ratio of 7:3 gave the most convenient spreading velocity for the time-lapse observation of an SLB, while 100% Egg-PG did not self-spread. Thus, we employed a molar ratio of 7:3 for all of the experiments. Fluorescence from the SLB was observed with a confocal laser scanning microscope. When the voltage (V) applied between the nanogap electrodes was 0 V, a single SLB developed along a microchannel from the left side. The SLB passed through the nanogap without spreading across the

Received: January 14, 2011
Published: April 05, 2011

dx.doi.org/10.1021/ja200367n | J. Am. Chem. Soc. 2011, 133, 6118–6121

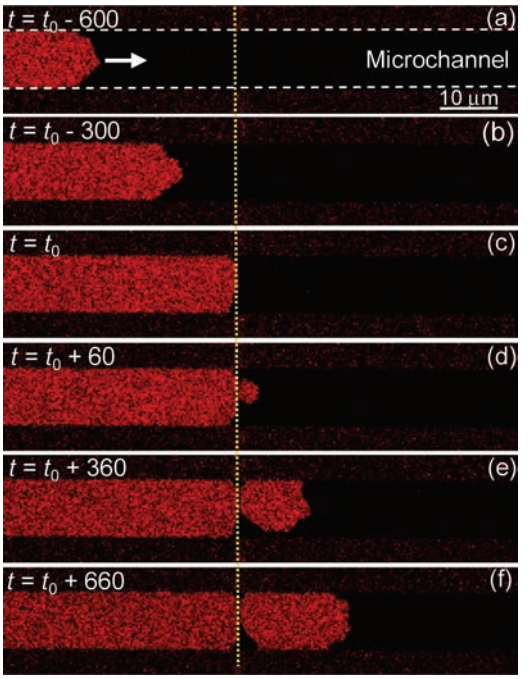

Figure 2. Time evolution of a self-spreading SLB before and after it passed through a nanogap. The applied voltage was −50 mV DC. A nanogap with a separation of 15 nm was used. The red areas in the microchannel were produced by fluorescence from the SLB, which included 1 mol % Texas Red−DHPE. The SLB grew from left to right along the microchannel. The yellow dotted line indicates the position of the nanogap. The time at which the advancing lipid bilayer reached the nanogap was set at $t = t_0$. (a) $t = t_0 - 600$ s; (b) $t = t_0 - 300$ s; (c) $t = t_0$; (d) $t = t_0 + 60$ s; (e) $t = t_0 + 360$ s; (f) $t = t_0 + 660$ s.

hydrophobic photoresist or gold patterns [see the Supporting Information (SI)].[10a]

When the applied voltage was not 0 V, the self-spreading behavior depended largely on the nanogap width. Figure 2 shows a typical time evolution for a self-spreading SLB using a nanogap with a separation of >10 nm. The red area in the microchannel shows the self-spreading SLB. The background red fluorescence surrounding the microchannel came from the organic photoresist forming the microchannel pattern, because the photoresist was fluorescent.[6,10] The time at which the advancing SLB reached the nanogap was set at $t = t_0$. Under this condition, the self-spreading behavior was almost the same with that for $V = 0$ V. No significant dependence on the applied voltage could be observed even when the SLB passed through the nanogap. Figure 3 shows a typical time evolution for a self-spreading SLB induced by the temporal switching of the applied voltage when we used a nanogap with a separation of <5 nm, which corresponded to the resolution limit of our scanning electron microscope. Before the SLB passed through the nanogap (Figure 3a,b), no voltage-dependent changes in the self-spreading were observed except in close proximity to the nanogap, as mentioned below. However, when the SLB reached the nanogap, the self-spreading was forcibly prevented by the application of −50 mV DC (Figure 3c). This continued for ∼300 s, corresponding to the interval of the voltage application (Figure 3d). Interestingly, the SLB started to develop again immediately after the applied voltage was returned to 0 V (Figure 3e−g). Furthermore, we confirmed that this ON/OFF switching of the self-spreading behavior could be

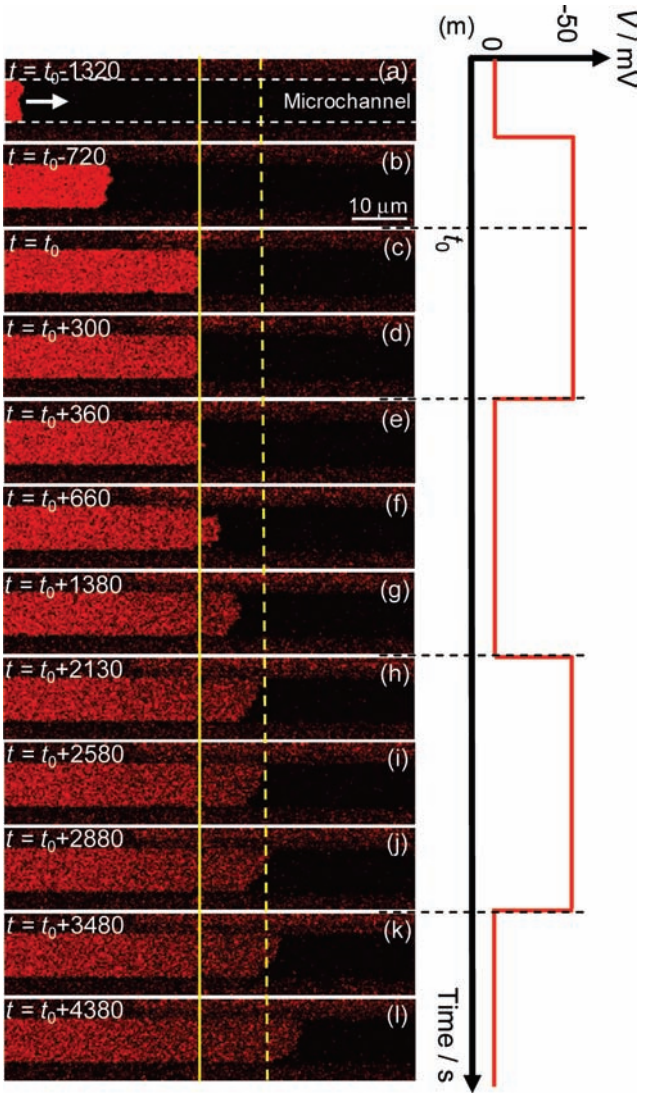

Figure 3. Time evolution of a self-spreading SLB before and after it passed through a nanogap induced by the temporal switching of the applied voltage. A nanogap with a separation of less than 5 nm was used. The red areas in the microchannel were produced by fluorescence from the SLB, which included 1 mol % Texas Red−DHPE. The SLB grew from left to right along the microchannel. Yellow solid and dotted lines indicate the position of the nanogap and the second pinning position of the SLB, respectively. The time at which the advancing lipid bilayer reached the nanogap was set at $t = t_0$. (a) $t = t_0 - 1320$ s; (b) $t = t_0 - 720$ s; (c) $t = t_0$; (d) $t = t_0 + 300$ s; (e) $t = t_0 + 360$ s; (f) $t = t_0 + 660$ s; (g) $t = t_0 + 1380$ s; (h) $t = t_0 + 2130$ s; (i) $t = t_0 + 2580$ s; (j) $t = t_0 + 2880$ s; (k) $t = t_0 + 3480$ s; (l) $t = t_0 + 4380$ s; (m) record of the voltage application. The time axis corresponds to the time at each image shown on the left.

repeatedly observed, corresponding to the temporal switching of the applied voltage (Figure 3h−l).

In regard to the self-spreading kinetics from a phenomenological point of view, application of an electric field to the nanogap did not affect the total energetic balance but did affect the local movement of lipid molecules around the nanogap. For the self-spreading, a continuous supply of molecules from a lipid source and a gain in the free energy of the SLB−substrate interaction are vital. Therefore, the electric field applied locally to a nanogap acted as a gate for the molecule supply.

dx.doi.org/10.1021/ja200367n |J. Am. Chem. Soc. 2011, 133, 6118–6121

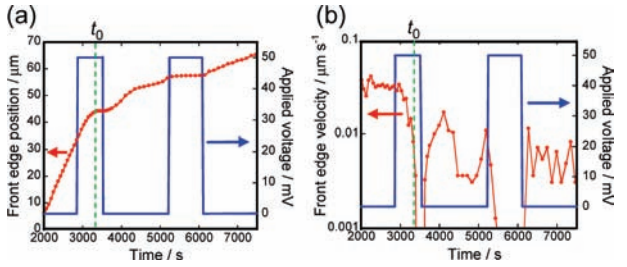

Figure 4. (a) Plots of the front-edge position of the SLB (red) and the applied voltage (blue) as functions of time. The green dotted line indicates the time at which the advancing SLB reached the nanogap. (b) Plots of the front-edge velocity of the SLB (red) and the applied voltage (blue) as functions of time.

Figure 4 shows plots of the front-edge position and velocity of the SLB derived from Figure 3 (red) and the applied voltage (blue) as a function of time. Green dotted lines show the time at which the advancing SLBs reached the nanogap. We can clearly see that once the front edge of the SLB had passed through the nanogap, the ON/OFF behavior of the SLB self-spreading corresponded completely to that of the applied voltage. An interesting point is that there was a sudden decrease in the front-edge velocity just before the SLB reached the nanogap. This implies that the front edge of the SLB could detect the existence of the nanogap despite the fact that it had not yet reached the nanogap. This is probably due to the electric flux around the nanogap.

The trapping of the SLB by the nanogap is reminiscent of electrostatic trapping, which has often been used to trap single molecules,[12] nanoparticles,[13] and even lipid vesicles[14] by employing the strong electric field generated in the nanospace. However, the situation is slightly different from that described in previous studies. Usually pure water or a dilute electrolyte solution is used for electrostatic trapping. In contrast, we used a dense electrolyte buffer solution, and therefore, the electric field was shielded by counterions except in close proximity to the electrode surface, known as the electric double layer. Taking our experimental conditions into account, we assumed that the electric double layer plays a complementary role in the trapping of SLBs. The electric double layer, which is characterized by the Debye length, is one of the key concepts for understanding nanometer-scale phenomena in solutions. For example, some interesting work on nanofluidic transistors[15] and ion-sensitive field-effect transistors for biomolecule sensing[16] has been reported. In regard to electrostatic trapping, the importance of the electric double layer was recently described in relation to the optical trapping of various nanometer-scale objects.[14]

For NaCl solutions, the Debye length (D) can be expressed as

$$D \approx \frac{0.304}{\sqrt{c}} \qquad (1)$$

where c the ionic concentration of NaCl.[17] Using eq 1, we estimated the width of the electric double layer to be ~1 nm under our experimental conditions. When the width of the nanogap is close to the order of the Debye length, the effect of applying a voltage is different from that in a bulk system, for which the nanogap width is sufficiently larger than the width of the electric double layer. Therefore, for a narrow nanogap with a separation of a few nanometers, the electric field can be effectively applied between the nanogap electrodes without being shielded by counterions as a result of the overlap of the two electric double layers. In such a situation, the electric field in the nanogap becomes large even when the applied voltage is several tens of millivolts (~10^5 V/cm). Thermodynamics implies that when an electric field is applied between nanogap electrodes, the energetic balance of a lipid molecule between diffusion within a two-dimensional SLB and the electrostatic force can be expressed as $2k_BT = qEd_B$, where k_B is the Boltzmann constant, T is the absolute temperature, q is the charge of the lipid molecule, E is the maximum electric field, and d_B is the amplitude of the Brownian motion within the SLB. Under our experimental conditions, where typically $q \approx e$ and $E \approx 10^5$ V/cm, this gives $d_B = 2k_BT/qE \approx 5$ nm. This suggests that the lipid molecule can fluctuate within at most 5 nm in the vicinity of the nanogap, leading to the electrostatic trapping of the charged lipid molecule. It should be noted that uncharged Egg-PC was also trapped by an electric field as well as charged Egg-PG and Texas Red−DHPE because the fluorescence image of the SLB in Figure 3 shows a clear front edge even after the SLB had passed through the nanogap. If uncharged Egg-PC passed through the nanogap without being trapped and formed a bilayer, charged lipids could diffuse into the label-free spreading bilayer after switching off, leading to a fluorescence image with an obscure front edge. It is thus plausible to think that the trapped molecules closed the nanogap gate, which prevented any lipid molecules from passing through it. There is another possibility, namely, that uncharged Egg-PC was trapped by an electric field because an amphiphilic lipid molecule has an electric dipole. Although the trapping mechanism remains unclear, we think that both steric and electric factors contribute to the trapping of uncharged lipid molecules. It should be also noted that the temporal switching response was fairly fast. Figure 3e shows a fluorescent image obtained just after the applied voltage was set at 0 V, where slight lipid molecule penetration was observed to the right of the nanogap spacing. This is evidence for the trapping of the SLB by the electric field.

As discussed above, we elucidated the trapping mechanism of an SLB in terms of the combination of an electric double layer and electrostatic trapping. The electric double layer thickness can be tuned by controlling the ionic concentration of the electrolyte. Therefore, as the next experimental step, we investigated the dependence of self-spreading on the ionic concentration of NaCl in a buffer solution as well as the width of the nanogap. We changed the initial ionic concentration of NaCl from 100 to 1 mM, which corresponds to $D \approx 10$ nm from eq 1. The other experimental conditions were exactly the same as those for 100 mM NaCl. When we used nanogaps with separations of <50 nm, we could control the development of the SLBs by the temporal switching of the applied voltage. In contrast, no significant effect was observed for nanogaps with separations of >60 nm (see the SI). It should be mentioned that 50 nm is slightly large in comparison with the sum of the Debye lengths from both electrode surfaces (~20 nm). To understand these phenomena more quantitatively, let us consider the electric potential in the nanogap. For a rough approximation using the Debye−Hückel equation,[17] the electric potential in the nanogap can be expressed as

$$\phi(x) = \phi_0\left[e^{-x/D} + e^{(x-d)/D}\right] \qquad (2)$$

where $\phi(x)$ is the electric potential at a distance x from one side of the electrode surfaces, ϕ_0 is the surface potential at the electrode, and d is the width of the nanogap. Figure 5 shows the results calculated from eq 2 under various experimental conditions. When the nanogap width is sufficiently greater than the Debye length, the

dx.doi.org/10.1021/ja200367n |J. Am. Chem. Soc. 2011, 133, 6118–6121

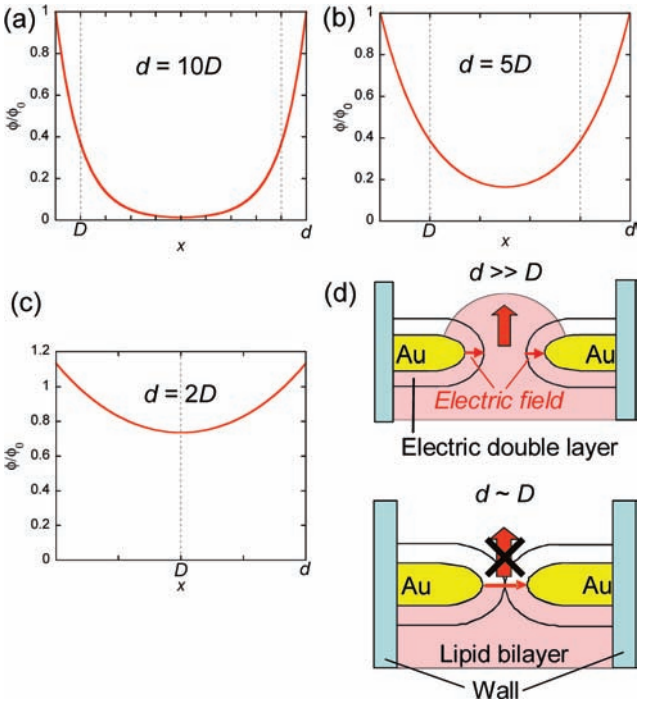

Figure 5. Calculated electric potentials in the nanogap. Dotted lines show the positions at the Debye length. (a) $d = 10D$ ($D = 1$ nm, $d = 10$ nm or $D = 10$ nm, $d = 100$ nm). (b) $d = 5D$ ($D = 1$ nm, $d = 5$ nm or $D = 10$ nm, $d = 50$ nm). (c) $d = 2D$ ($D = 10$ nm, $d = 20$ nm). (d) Schematic images of electrostatic trapping.

electric potential decays exponentially to zero over a distance on the order of the Debye length (Figure 5a). Therefore, electrostatic control of the SLB self-spreading is impossible, as illustrated in the upper part of Figure 5d. In contrast, when the sum of the Debye lengths is on the order of the width of the nanogap, the electric potential even at the center of the nanogap has a nonzero value (Figure 5b,c). The electric field can penetrate throughout the nanogap, enabling direct control of the SLB self-spreading, as illustrated in the lower part of Figure 5d. This result is in good agreement with the experimental results (see the SI). It is noteworthy that ON/OFF switching of the self-spreading was achieved even under such conditions as $D = 10$ nm and $d = 50$ nm.

In conclusion, we have investigated the effect of an external electric field applied to SLBs passing through a nanogap gate and demonstrated for the first time that the development of the SLBs can be controlled by the temporal switching of the applied electric field. We have revealed that the electric double layer plays a crucial role in this behavior in conjunction with the electrostatic trapping of the SLB between the nanogap electrodes. The validity of this mechanism was confirmed by the dependence of the self-spreading on the nanogap width and the ionic concentration of NaCl. The technique described here constitutes the first demonstration of the temporal and spatial control of biomembrane development in a nanometer-scale device and can provide new opportunities for the realization of nanobio devices and the study of nanofluidics.

■ ASSOCIATED CONTENT

Ⓢ Supporting Information. Detailed experimental methods, control measurement without voltage application, and results for the ionic concentration dependence. This material is available free of charge via the Internet at http://pubs.acs.org.

■ AUTHOR INFORMATION

Corresponding Author
kasimura@nttbrl.jp

■ ACKNOWLEDGMENT

This work was supported by a Grant-in-Aid for Scientific Research from the Japan Society for the Promotion of Science (20310076).

■ REFERENCES

(1) Sackmann, E. *Science* **1996**, *271*, 43.
(2) Groves, J. T.; Boxer, S. G. *Acc. Chem. Res.* **2002**, *35*, 149.
(3) (a) Groves, J. T.; Boxer, S. G. *Biophys. J.* **1995**, *69*, 1972. (b) Groves, J. T.; Boxer, S. G.; McConnell, H. M. *Proc. Natl. Acad. Sci. U.S.A.* **1997**, *94*, 13390. (c) Groves, J. T.; Boxer, S. G.; McConnell, H. M. *Proc. Natl. Acad. Sci. U.S.A.* **1998**, *95*, 935. (d) Grogan, M. J.; Kaizuka, Y.; Conrad, R. M.; Groves, J. T.; Bertozzi, C. R. *J. Am. Chem. Soc.* **2005**, *127*, 14383.
(4) van Oudenaarden, A.; Boxer, S. G. *Science* **1999**, *285*, 1046.
(5) (a) Daniel, S.; Diaz, A. J.; Martinez, K. M.; Bench, B. J.; Albertorio, F.; Cremer, P. S. *J. Am. Chem. Soc.* **2007**, *129*, 8072. (b) Jackson, B. L.; Nye, J. A.; Groves, J. T. *Langmuir* **2008**, *24*, 6189. (c) Groves, J. T.; Wülfing, C.; Boxer, S. G. *Biophys. J.* **1996**, *71*, 2716. (d) Groves, J. T.; Boxer, S. G.; McConnell, H. M. *J. Phys. Chem. B* **2000**, *104*, 11409.
(6) Furukawa, K.; Nakashima, H.; Kashimura, Y.; Torimitsu, K. *Lab Chip* **2006**, *6*, 1001.
(7) (a) Rädler, J.; Strey, H.; Sackmann, E. *Langmuir* **1995**, *11*, 4539. (b) Nissen, J.; Gritsch, S.; Wiegand, G.; Rädler, J. O. *Eur. Phys. J. B* **1999**, *10*, 335. (c) Furukawa, K.; Sumitomo, K.; Nakashima, H.; Kashimura, Y.; Torimitsu, K. *Langmuir* **2007**, *23*, 367.
(8) (a) Nabika, H.; Sasaki, A.; Takimoto, B.; Sawai, Y.; He, S.; Murakoshi, K. *J. Am. Chem. Soc.* **2005**, *127*, 16786. (b) Nabika, H.; Iijima, N.; Takimoto, B.; Ueno, K.; Misawa, H.; Murakoshi, K. *Anal. Chem.* **2009**, *81*, 699.
(9) Furukawa, K.; Nakashima, H.; Kashimura, Y.; Torimitsu, K. *Langmuir* **2008**, *24*, 921.
(10) (a) Kashimura, Y.; Durao, J.; Furukawa, K.; Torimitsu, K. *Jpn. J. Appl. Phys.* **2008**, *47*, 3248. (b) Kashimura, Y.; Furukawa, K.; Torimitsu, K. *Jpn. J. Appl. Phys.* **2010**, *49*, No. 04DL15.
(11) Texas Red−DHPE: Texas Red−1,2-dihexadecanoyl-*sn*-glycero-3-phosphoethanolamine, triethylammonium salt.
(12) Porath, D.; Bezryadin, A.; de Vries, S.; Dekker, C. *Nature* **2000**, *403*, 635.
(13) (a) Bezryadin, A.; Dekker, C.; Schmid, G. *Appl. Phys. Lett.* **1997**, *71*, 1273. (b) Bezryadin, A.; Dekker, C. *J. Vac. Sci. Technol., B* **1997**, *15*, 793.
(14) Krishnan, M.; Mojarad, N.; Kukura, P.; Sandoghdar, V. *Nature* **2010**, *467*, 692.
(15) (a) Daiguji, H.; Yang, P.; Majumdar, A. *Nano Lett.* **2004**, *4*, 137. (b) Karnik, R.; Fan, R.; Yue, M.; Li, D.; Yang, P.; Majumdar, A. *Nano Lett.* **2005**, *5*, 943. (c) Karnik, R.; Castelino, K.; Majumdar, A. *Appl. Phys. Lett.* **2006**, *88*, No. 123114.
(16) Sakata, T.; Miyahara, Y. *Biosens. Bioelectron.* **2007**, *22*, 1311.
(17) Israelachvili, J. N. *Intermolecular and Surface Forces*, 2nd ed.; Academic Press: London, 1992; Chapter 12.